



**Oceanic bromine emissions weighted by their ozone depletion potential**

S. Tegtmeier et al.

This discussion paper is/has been under review for the journal Atmospheric Chemistry and Physics (ACP). Please refer to the corresponding final paper in ACP if available.

# Oceanic bromine emissions weighted by their ozone depletion potential

S. Tegtmeier<sup>1</sup>, F. Ziska<sup>1</sup>, I. Pisso<sup>2</sup>, B. Quack<sup>1</sup>, G. J. M. Velders<sup>3</sup>, X. Yang<sup>4</sup>, and K. Krüger<sup>5</sup>

<sup>1</sup>GEOMAR Helmholtz Centre for Ocean Research Kiel, Kiel, Germany

<sup>2</sup>Norwegian Institute for Air Research (NILU), Kjeller, Norway

<sup>3</sup>National Institute for Public Health and the Environment, Bilthoven, the Netherlands

<sup>4</sup>British Antarctic Survey, Cambridge, UK

<sup>5</sup>University of Oslo, Oslo, Norway

Received: 12 March 2015 – Accepted: 2 May 2015 – Published: 26 May 2015

Correspondence to: S. Tegtmeier (stegtmeier@geomar.de)

Published by Copernicus Publications on behalf of the European Geosciences Union.

Title Page

Abstract

Introduction

Conclusions

References

Tables

Figures



Back

Close

Full Screen / Esc

Printer-friendly Version

Interactive Discussion



## Abstract

At present, anthropogenic halogens and oceanic emissions of Very Short-Lived Substances (VSLS) are responsible for stratospheric ozone destruction. Emissions of the, mostly long-lived, anthropogenic halogens have been reduced, and as a consequence, their atmospheric abundance has started to decline since the beginning of the 21st century. Emissions of VSLS are, on the other hand, expected to increase in the future. VSLS are known to have large natural sources; however increasing evidence arises that their oceanic production and emission is enhanced by anthropogenic activities. Here, we introduce a new approach of assessing the overall impact of all oceanic halogen emissions on stratospheric ozone by calculating Ozone Depletion Potential (ODP)-weighted emissions of VSLS. Seasonally and spatially dependent, global distributions are derived exemplary for  $\text{CHBr}_3$  for the period 1999–2006. At present, ODP-weighted emissions of  $\text{CHBr}_3$  amount up to 50 % of ODP-weighted anthropogenic emissions of CFC-11 and to 9 % of all long-lived ozone depleting substances. The ODP-weighted emissions are large where strong oceanic emissions coincide with high-reaching convective activity and show pronounced peaks at the equator and the coasts with largest contributions from the Maritime Continent and West Pacific. Variations of tropical convective activity lead to seasonal shifts in the spatial distribution of the ODP with the updraught mass flux explaining 71 % of the variance of the ODP distribution. Future climate projections based on RCP8.5 scenario suggest a 31 % increase of the ODP-weighted  $\text{CHBr}_3$  emissions until 2100 compared to present values. This increase is related to larger convective activity and increasing emissions in a future climate; however, is reduced at the same time by less effective bromine-related ozone depletion. The comparison of the ODP-weighted emissions of short and long-lived halocarbons provides a new concept for assessing the overall impact of oceanic bromine emissions on stratospheric ozone depletion for current conditions and future projections.

## Oceanic bromine emissions weighted by their ozone depletion potential

S. Tegtmeier et al.

Title Page

Abstract

Introduction

Conclusions

References

Tables

Figures



Back

Close

Full Screen / Esc

Printer-friendly Version

Interactive Discussion





**Oceanic bromine emissions weighted by their ozone depletion potential**

S. Tegtmeier et al.

Title Page

Abstract

Introduction

Conclusions

References

Tables

Figures



Back

Close

Full Screen / Esc

Printer-friendly Version

Interactive Discussion



5 timates of 4 ppt (Hossaini et al., 2013), 4.5–6 ppt (Aschmann and Sinnhuber, 2013) and 7.7 ppt (Liang et al., 2014). The most abundant bromine containing VSLs are dibromomethane ( $\text{CH}_2\text{Br}_2$ ) and bromoform ( $\text{CHBr}_3$ ) with potentially important source regions in tropical, subtropical and shelf waters (Quack et al., 2007). The contribution of VSLs to stratospheric bromine in form of organic source gases or inorganic product gases depends strongly on the efficiency of troposphere–stratosphere transport compared to the photochemical loss of the source gases and to the wet deposition of the product gases. Uncertainties in the contribution of VSLs to stratospheric halogen loading mainly result from uncertainties in the emission inventories and from uncertainties in the modeled transport and wet deposition processes.

10 The relative contribution of individual halogens to stratospheric ozone depletion is often quantified by the Ozone Depletion Potential (ODP) defined as the time-integrated ozone depletion resulting from a unit mass emission of that substance relative to the ozone depletion resulting from a unit mass emission of CFC-11 ( $\text{CCl}_3\text{F}$ ) (Wuebbles, 1983). Ozone depletion and thus the definition of the ODP refer to anthropogenically emitted halogens. The ODP is independent of the total amount of the substance emitted and describes only the potential and not the actual damaging effect of the substance to the ozone layer, relative to that of CFC-11. While the ODP of long-lived halocarbons is a well-established and extensively used measure and plays an important role in the Montreal Protocol for control measures and reporting of emissions, the same concept can not easily be applied to shorter-lived substances. Despite, the ODP being traditionally defined for anthropogenic, long-lived halogens, some recent studies have applied the same concept to VSLs (e.g. Brioude et al., 2010; Pisso et al., 2010), which have also natural sources. Depending on the meteorological conditions, only a fraction of the originally released VSLs reach the stratosphere. As a consequence the ODP of a VSLs cannot be given as one number as for long-lived halocarbons but needs to be estimated as a function of time and location of emission. So far ODPs of VSLs have been estimated based on Eulerian (Wuebbles et al., 2001) and Lagrangian (Brioude et al., 2010; Pisso et al., 2010) studies, showing strong geographical and seasonal





**Oceanic bromine emissions weighted by their ozone depletion potential**

S. Tegtmeier et al.

Title Page

Abstract

Introduction

Conclusions

References

Tables

Figures

◀

▶

◀

▶

Back

Close

Full Screen / Esc

Printer-friendly Version

Interactive Discussion



et al., 2011) for 1979–2013 under the assumption that the constant concentration maps can be applied to the complete time period (Ziska et al., 2013). Recent model studies showed that atmospheric  $\text{CHBr}_3$  derived from the Ziska et al. (2013) bottom-up emission inventory agrees better with tropical aircraft measurements than other  $\text{CHBr}_3$  model estimates derived from top-down emission inventories (Hossaini et al., 2013).

Future emission estimates are calculated based on the present day (1989–2011) climatological concentration maps and future estimates of global sea surface temperature, pressure, winds and salinity (Ziska et al., 2015). The meteorological parameters are model output from the Community Earth System Model version 1 – Community Atmospheric Model version 5 (CESM1-CAM5) (Neale et al., 2010) runs based on the Representative Concentration Pathways (RCP) 8.5 scenarios conducted within phase 5 of the Coupled Model Intercomparison Project (CMIP5) (Taylor et al., 2012). The CESM1-CAM5 model has been chosen since it provides model output for all the parameters required to calculate future VLS emissions and future ODP estimates (Sect. 2.2). Comparisons have shown that the global emissions based on historical CESM1-CAM5 meteorological data agree well with emissions based on ERA-Interim fields (Ziska et al., 2015). The future global  $\text{CHBr}_3$  emissions increase by about 30 % until 2100 for the CESM1-CAM5 RCP8.5 simulation. These derived changes of the future VLS emissions are only driven by projected changes in the meteorological and marine surface parameters, but do not take into account possible changes of the oceanic concentrations, which will be assessed in follow-up studies.

## 2.2 $\text{CHBr}_3$ trajectory-derived ODP

The Ozone Depletion Potential is a measure of a substance's destructive effect to the ozone layer relative to the reference substance CFC-11 ( $\text{CCl}_3\text{F}$ ). ODPs of long-lived halogen compounds can be calculated based on the change in total ozone per unit mass emission of this compound using atmospheric chemistry-transport models. Alternatively, the ODP of a long lived species  $X$  can be estimated by a semi-empirical approach (Solomon et al., 1992):







2009). A more detailed derivation of the approximations and parameterizations including a discussion of the errors involved can be found in Pisso et al. (2010).

### 2.3 CHBr<sub>3</sub> mass flux-derived ODP

While present day ODP estimates for VSLs based on ERA-Interim are available (e.g. Pisso et al., 2010), the trajectory-based method has not been applied to future model scenarios so far. Therefore, we attempt to determine an ODP proxy easily available from climate model output, which can be used to derive future estimates of the ODP fields. In general, the ODP of a VSL as a function of time and location of emission is determined by tropospheric and stratospheric chemistry and transport processes. It has been shown, however, that the effect of spatial variations in the stratospheric residence time on the ODP is relatively weak (Pisso et al., 2010). We identify a pronounced relationship between the ODP of CHBr<sub>3</sub> and deep convective activity, which demonstrates that for such short-lived substances the ODP variability is mostly determined by the tropospheric transport processes. Based on the identified relationship we develop a proxy for the ODP of CHBr<sub>3</sub> based on the ERA-Interim convective upward mass flux. For the available trajectory-derived ODP fields, we determine a linear fit [ $a_0, a_1$ ] in a least-square sense:

$$y = a_0 + a_1 x + \varepsilon. \quad (2)$$

The dependent variable  $y$  is the trajectory-based ODP prescribed as a vector of all available monthly mean ODP values comprising 26 months of data re-gridded to the ERA-Interim standard resolution of  $1^\circ \times 1^\circ$ . The independent variable  $x$  is a vector of the ERA-Interim monthly mean updraught mass flux between 250 and 80 hPa with a  $1^\circ \times 1^\circ$  resolution for the same months. The fit coefficients [ $a_0, a_1$ ] are used to calculate the ODP proxy  $\hat{y}$

$$\hat{y} = a_0 + a_1 x. \quad (3)$$

## Oceanic bromine emissions weighted by their ozone depletion potential

S. Tegtmeier et al.

Title Page

Abstract

Introduction

Conclusions

References

Tables

Figures



Back

Close

Full Screen / Esc

Printer-friendly Version

Interactive Discussion







and a reduced effectiveness of bromine-related ozone depletion. Stratospheric chlorine in 1979 equals roughly the value expected for 2060 (Harris and Wuebbles, 2014), thus corresponding to a 13% reduced bromine  $\alpha$ -factor of 52. ODP values between 1979 and the year 1996, when the amount of stratospheric chlorine reached a peak and started to level off (Carpenter and Reimann, 2014), are estimated based on a linear interpolation over this time period.

## 2.4 ODP-weighted $\text{CHBr}_3$ emissions

The concept of ODP-weighted emissions combines information on the emission strength and on the relative ozone-destroying capability of a substance. Its application to VSLS has been recently rendered possible by the availability of observation-based VSLS emission maps (Ziska et al., 2013). Here, we calculate the present-day ODP-weighted emissions of  $\text{CHBr}_3$  for data available for four months (March, June, September and December) from 1999 to 2006 by multiplying the  $\text{CHBr}_3$  emissions with the trajectory-derived ODP at each grid point. The resulting ODP-weighted emission maps are given as a function of time (monthly averages) and location ( $1^\circ \times 1^\circ$  grid). Global annual means are calculated by averaging over all grid points and over the four given months.

In order to extend the time series of ODP-weighted  $\text{CHBr}_3$  emission beyond 1999 and 2006, we derive ODP fields from the ERA-Interim upward mass flux. The method is based on the polynomial fit determined for the available trajectory-derived  $\text{CHBr}_3$  ODP fields as described in Sect. 2.3. Multiplying the mass flux-derived ODP fields with the monthly mean emission fields from Ziska et al. (2013) results in a long term time series (1979–2013) of ODP-weighted  $\text{CHBr}_3$  emissions. Similarly, we use the CESM-CAM5 mass flux-derived ODP fields together with emission inventories derived from CESM-CAM5 meteorological data to produce historical (1979–2005) and future (2006–2100) model-driven ODP-weighted  $\text{CHBr}_3$  emission fields.

### Oceanic bromine emissions weighted by their ozone depletion potential

S. Tegtmeier et al.

Title Page

Abstract

Introduction

Conclusions

References

Tables

Figures



Back

Close

Full Screen / Esc

Printer-friendly Version

Interactive Discussion



### 3 ODP-weighted $\text{CHBr}_3$ emissions for present day conditions

We will introduce the concept of the ODP-weighted emissions of  $\text{CHBr}_3$  exemplarily for March 2005 and discuss how the ODP-weighted emissions of this very short-lived compound compare to those of long-lived halogens. The  $\text{CHBr}_3$  emissions (Ziska et al., 2013) for March 2005 are shown in Fig. 1a with highest emissions in coastal regions, in the upwelling equatorial waters and the Northern Hemisphere (NH) mid-latitude Atlantic. The emissions show large variations and reach values higher than  $1500 \text{ pmol m}^{-2} \text{ h}^{-1}$  in coastal regions characterized by high concentrations due to biological productivity and anthropogenic activities. In the tropical open ocean, emissions are often below  $100 \text{ pmol m}^{-2} \text{ h}^{-1}$ , while in the subtropical gyre regions, ocean and atmosphere are nearly in equilibrium and fluxes are around zero. Globally, the coastal and shelf regions account for about 80% of all  $\text{CHBr}_3$  emissions. Apart from the gradients between coastal, shelf and deep ocean waters the emissions show no pronounced longitudinal variations. Negative emissions occur in parts of the Southern Ocean, northern Pacific and North Atlantic and indicate a  $\text{CHBr}_3$  sink given by a flux from the atmosphere into the ocean.

The potentially damaging effect of  $\text{CHBr}_3$  on the stratospheric ozone layer is displayed in Fig. 1b in form of the ODP of  $\text{CHBr}_3$  given as a function of time and location of the emission but independent of its strength. Overall, the ODP of  $\text{CHBr}_3$  is largest in the tropics (tropical ODP belt) and has low values (mostly below 0.1) north and south of  $20^\circ$ . The ODP depends strongly on the efficiency of rapid transport from the surface to the stratosphere which is in turn determined by the intensity of high reaching convection. In the NH winter/spring of most years, the strongest convection and therefore the highest ODP values of up to 0.85 are found over the equatorial West Pacific (Pisso et al., 2010). In contrast to the  $\text{CHBr}_3$  emission estimates, the ODP shows pronounced longitudinal variations linked to the distribution of convection and low-level flow patterns.

## Oceanic bromine emissions weighted by their ozone depletion potential

S. Tegtmeier et al.

Title Page

Abstract

Introduction

Conclusions

References

Tables

Figures



Back

Close

Full Screen / Esc

Printer-friendly Version

Interactive Discussion





**Oceanic bromine emissions weighted by their ozone depletion potential**

S. Tegtmeier et al.

Title Page

Abstract

Introduction

Conclusions

References

Tables

Figures



Back

Close

Full Screen / Esc

Printer-friendly Version

Interactive Discussion

in less than 10% over the globe, the relatively large  $\text{CHBr}_3$  emissions make up for the mostly small ODP. Current estimates of global  $\text{CHBr}_3$  emissions range between 249 and  $864 \text{ Ggyr}^{-1}$  (Ziska et al., 2013 and references therein), with the higher global emission estimates coming from top-down methods while the lower boundary is given by the bottom-up study from Ziska et al. (2013). Already this lower boundary of the unweighted  $\text{CHBr}_3$  emissions, exceeds the combined emissions of the most abundant CFCs. For our study, even the choice of the lowest emission inventory leads to relatively large ODP-weighted emissions of the very short-lived  $\text{CHBr}_3$  as discussed above. Choosing a different emission inventory than Ziska et al. (2013) would result in even larger ODP-weighted  $\text{CHBr}_3$  emissions. Still more important than the overall  $\text{CHBr}_3$  emission strength is the fact that emission and ODP show the same latitudinal gradients with both fields having higher values at the low latitudes. This spatial coincidence of large sources and efficient transport causes the relatively large global mean value of ODP-weighted  $\text{CHBr}_3$  emissions.

It is important to keep in mind that the long-lived halocarbons are to a large degree of anthropogenic origin, while  $\text{CHBr}_3$  is believed to have mostly natural sources. However,  $\text{CHBr}_3$  in coastal regions also results from anthropogenic activities such as aqua-farming in South-East Asia (Leedham et al., 2013) and oxidative water treatment (Quack and Wallace, 2003). While these sources accounted for only a small fraction of the global budget in 2003 (Quack and Wallace, 2003), their impact is currently increasing. Since the general ODP concept has been originally defined for anthropogenic halogens, the ODP-weighted  $\text{CHBr}_3$  emissions should be calculated only for the anthropogenic component of the emissions. However, since no such estimates are available at the moment, the method will be applied to the combined emission field. Given that the natural oceanic production and emission of halogenated VSLs are expected to change in the future due to increasing ocean acidification, changing primary production and ocean surface meteorology (Hepach et al., 2014), it will remain a huge challenge to properly separate natural and anthropogenic emissions of these gases.



## 4 ODP proxy

It is necessary to understand the short and long-term changes of the ODP-weighted  $\text{CHBr}_3$  emissions in order to predict their future development. On the seasonal time scales, the ODP-weighted  $\text{CHBr}_3$  emissions show large variations as demonstrated in Fig. 4 for June and December 2001. In the NH summer, 57% of the ODP-weighted emissions stem from the NH tropical belt (30–0° N) with largest contributions from the Maritime Continent and Asian coastal areas. In the NH winter, the ODP-weighted emissions shift to the SH tropical belt (48%) with strongest contributions from the West Pacific. While the Maritime Continent is an important source region all-year around, emissions from the southern coast line of Asia during NH winter are not very important for stratospheric ozone depletion. The emissions reveal slight seasonal variations (not shown here) due to varying surface wind and sea surface temperature; however, it is the seasonality of the ODP (Fig. 5a) that causes the pronounced shift of the ODP-weighted emissions from one hemisphere to the other.

We want to analyze the long-term changes of ODP-weighted  $\text{CHBr}_3$  emission and thus need to extend the time series beyond 1999 and 2006. While  $\text{CHBr}_3$  emissions are available for 1979–2013, the ODP itself, based on costly trajectory calculations, is restricted to 1999–2006. In order to develop an ODP proxy, we analyze in a first step the variations of the trajectory-derived ODP fields and their relation to meteorological parameters. The ODP fields for the months June and December 2001 shown in Fig. 5a have their maxima between 0 and 20° N for the NH summer and 5° N and 15° S for the NH winter. In the NH summer, the dominant source region for stratospheric  $\text{CHBr}_3$  is located in the equatorial West Pacific region including south-east Asia. In the NH winter, the source region is shifted westward and southward with its center now over the West Pacific. These seasonal variations agree with results from previous trajectory studies (e.g. Fueglistaler et al., 2005; Krüger et al., 2008) and are consistent with the main patterns of tropical convection (Gettelman et al., 2002).

### Oceanic bromine emissions weighted by their ozone depletion potential

S. Tegtmeier et al.

Title Page

Abstract

Introduction

Conclusions

References

Tables

Figures



Back

Close

Full Screen / Esc

Printer-friendly Version

Interactive Discussion



**Oceanic bromine emissions weighted by their ozone depletion potential**

S. Tegtmeier et al.

Title Page

Abstract

Introduction

Conclusions

References

Tables

Figures



Back

Close

Full Screen / Esc

Printer-friendly Version

Interactive Discussion



A detailed picture of the high reaching convective activities within these two months is given in Fig. 5b in form of the ERA-Interim monthly mean updraught mass flux between 250 and 80 hPa. The rapid updraughts transporting air masses from the boundary layer into the tropical tropopause layer (TTL) are part of the ascending branch of the tropospheric circulation constituted by the position of the intertropical convergence zone (ITCZ). The updraught convective mass fluxes are largest in and near the summer monsoon driven circulations close to the equator. Over the West Pacific and Maritime Continent the region of intense convection is quite broad compared to the other ocean basins due to the large oceanic warm pool and strong monsoon flow. In addition to the overall annual north–south migration pattern, large seasonal changes of the updraught mass flux are visible over South America and the Maritime Continent consistent with the climatological distribution of the ITCZ. The south-east ward pointing extension in the Pacific is strongest in the NH winter and indicates a double ITCZ.

We derive a  $\text{CHBr}_3$  ODP proxy from the ERA-Interim updraught mass fluxes (referred to as mass flux-derived ODP, see Sect. 2.3 for details). The strong correlation between  $\text{CHBr}_3$  ODP and high-reaching convection justifies our method by indicating that variations in chemistry or stratospheric residence time have only minor impact on the ODP variability. The mass flux-derived ODP fields are shown in Fig. 5c and explain 76 and 81 % of the variance of the original trajectory-derived ODP fields (Fig. 5a). Differences between the trajectory-derived ODP fields and the mass flux-derived proxy may be caused by the fact that not only the location of the most active convective region will determine the ODP distribution but also patterns of low-level flow into these regions. Additionally, spatial and seasonal variations in the expected stratospheric residence time may have a small impact on the trajectory-derived ODP and cause deviations to the mass flux-derived proxy. Largest disagreement between the trajectory-derived and mass flux-derived ODP is found over South America and Africa. However, the ODP values over the continents are not important for the ODP-weighted  $\text{CHBr}_3$  emissions due to the very low to non-existent emissions over land (Quack and Wallace, 2003) and are not used in our study.









parameterization of deep convection and ENSO simulation (Neale et al., 2008). Overall, our analysis demonstrates that the spatial and seasonal variability of the model fields allows to derived realistic ODP-weighted  $\text{CHBr}_3$  emission estimates.

## 7 ODP-weighted $\text{CHBr}_3$ emissions for 2006–2100

Future ODP-weighted  $\text{CHBr}_3$  emissions shown in Fig. 10a are based on future model estimates of the  $\text{CHBr}_3$  emission and the  $\text{CHBr}_3$  ODP proxy. Both quantities are calculated based on the meteorological and marine surface variables and convective mass flux from the CESM1-CAM5, RCP8.5 runs. In addition, we have applied a correction factor to the ODP fields to account for a changing  $\alpha$ -factor based on less effective ozone loss cycles in the stratosphere given the decrease of anthropogenic chlorine (Sect. 2.3). The future estimates of the ODP-weighted  $\text{CHBr}_3$  emissions show pronounced interannual variations of up to 20%. Overall, the ODP-weighted emissions increase steadily until 2100 by about 31% of the 2006–2015 mean value corresponding to a linear trend of  $2.6\% \text{decade}^{-1}$ .

In order to analyze what causes the strong interannual variability and the long-term trend, we conduct sensitivity studies where only one factor (emissions, mass flux-derived ODP, stratospheric chemistry) is changing while the other two are kept constant. Figure 10b displays the time series of ODP-weighted  $\text{CHBr}_3$  emissions for varying oceanic emission fields. The emission-driven time series for 2006–2100 shows a positive trend of  $2.2\% \text{decade}^{-1}$  which is in the range of the trend observed for the emission-driven time series for 1979–2013 based on ERA-Interim (Fig. 7b). However, the model-based ODP-weighted emissions show no long-term change over the first 15 years and the positive, emission-driven trend only starts after 2020. The second sensitivity study (Fig. 10c) highlights changes in the ODP-weighted emissions attributable to high-reaching convection (via the mass flux-derived ODP), while emission fields and  $\alpha$ -factor are kept constant. Clearly, the strong interannual variations in the combined time series (Fig. 10a) are caused by the same fluctuations in the mass flux-

### Oceanic bromine emissions weighted by their ozone depletion potential

S. Tegtmeier et al.

Title Page

Abstract

Introduction

Conclusions

References

Tables

Figures



Back

Close

Full Screen / Esc

Printer-friendly Version

Interactive Discussion











**Oceanic bromine emissions weighted by their ozone depletion potential**

S. Tegtmeier et al.

Title Page

Abstract

Introduction

Conclusions

References

Tables

Figures



Back

Close

Full Screen / Esc

Printer-friendly Version

Interactive Discussion



creasing  $\text{CHBr}_3$  emissions and further amplify the importance of VLSL for stratospheric ozone chemistry. Such changes in the oceanic sources are important for estimating the future impact of VLSL on atmospheric processes, but are not well enough understood yet to derive reliable future projections. Some discrepancies between the observation- and model-derived ODP-weighted  $\text{CHBr}_3$  emissions exist, very likely related to out of phase tropical meteorology in the model. However, overall, there is a good agreement between the spatial and seasonal variability of the observation- and model-derived fields giving us confidence to use this model in order to derived realistic ODP-weighted  $\text{CHBr}_3$  emission estimates.

Variability of the ODP-weighted  $\text{CHBr}_3$  emissions on different time scales are driven by different processes. Spatial and seasonal variations are caused by variations in the surface to tropopause transport via deep convection. Inter-annual variability is mostly driven by transport but also by the variability in the oceanic emissions. Both processes are weakly correlated on inter-annual time scales (with a Pearson correlation coefficient between the interannual anomalies of  $r = 0.3$ ), suggesting that in years with stronger emissions (driven by stronger surface winds and higher temperatures) stronger troposphere–stratosphere transport exist. The long-term trend, finally, can be attributed in equal parts to changes in emissions, tropospheric transport and stratospheric chemistry. While growing oceanic emissions and changing convective activity lead to increasing ODP-weighted  $\text{CHBr}_3$  emissions, the expected decline in stratospheric chlorine background levels has the opposite effect and leads to a decrease. Taking all three processes into account, the future model projections suggest a 31 % increase of the ODP-weighted  $\text{CHBr}_3$  emissions until 2100 for the RCP8.5 scenario. This anthropogenically driven increase will further enhance the importance of  $\text{CHBr}_3$  for stratospheric ozone chemistry.

*Acknowledgements.* The authors are grateful to the ECMWF for making the reanalysis product ERA-Interim available. This study is carried out within the EU project SHIVA (FP7-ENV-2007-1-226224) and the BMBF project ROMIC THREAT (01LG1217A). We thank Steve Montzka for helpful discussions.

The article processing charges for this open-access publication were covered by a Research Centre of the Helmholtz Association.

## References

- 5 Aschmann, J. and Sinnhuber, B.-M.: Contribution of very short-lived substances to stratospheric bromine loading: uncertainties and constraints, *Atmos. Chem. Phys.*, 13, 1203–1219, doi:10.5194/acp-13-1203-2013, 2013.
- Austin, J., N. and Butchart, N.: Coupled chemistry-climate model simulations for the period 1980 to 2020: ozone depletion and the start of ozone recovery, *Q. J. Roy. Meteorol. Soc.*, 129, 3225–3249, 2006.
- 10 Brioude, J., Portmann, R. W., Daniel, J. S., Cooper, O. R., Frost, G. J., Rosenlof, K. H., Granier, C., Ravishankara, A. R., Montzka, S. A., and Stohl, A.: Variations in ozone depletion potentials of very short-lived substances with season and emission region, *Geophys. Res. Lett.*, 37, L19804, doi:10.1029/2010GL044856, 2010.
- 15 Butchart, N.: The Brewer–Dobson circulation, *Rev. Geophys.*, 52, 157–184, doi:10.1002/2013RG000448, 2014.
- Carpenter, L. J. (lead author), Reimann, S. (lead author), Burkholder, J. B., Clerbaux, C., Hall, B. D., Hossaini, R., Laube, J. C., and Yvon-Lewis, S. A.: Ozone-Depleting Substances (ODSs) and Other Gases of Interest to the Montreal Protocol, in: Chapter 1 in *Scientific Assessment of Ozone Depletion: 2014*, Global Ozone Research and Monitoring Project–Report No. 55, World Meteorological Organization, Geneva, Switzerland, 2014.
- 20 Daniel, J. S., Solomon, S., Portmann, R. W., and Garcia, R. R.: Stratospheric ozone destruction: the importance of bromine relative to chlorine, *J. Geophys. Res.*, 104, 23871–23880, 1999.
- Dee, D. P., Uppala, S. M., Simmons, A. J., Berrisford, P., Poli, P., Kobayashi, S., Andrae, U., 25 Balmaseda, M. A., Balsamo, G., Bauer, P., Bechtold, P., Beljaars, A. C. M., van de Berg, L., Bidlot, J., Bormann, N., Delsol, C., Dragani, R., Fuentes, M., Geer, A. J., Haimberger, L., Healy, S. B., Hersbach, H., Hólm, E. V., Isaksen, L., Kållberg, P., Köhler, M., Matricardi, M., McNally, A. P., Monge-Sanz, B. M., Morcrette, J.-J., Park, B.-K., Peubey, C., de Rosnay, P., Tavolato, C., Thépaut, J.-N. and Vitart, F.: The ERA-Interim reanalysis: configuration and performance of the data assimilation system, *Q. J. Roy. Meteorol. Soc.*, 137, 553–597, 30 doi:10.1002/qj.828, 2011.

## Oceanic bromine emissions weighted by their ozone depletion potential

S. Tegtmeier et al.

Title Page

Abstract

Introduction

Conclusions

References

Tables

Figures



Back

Close

Full Screen / Esc

Printer-friendly Version

Interactive Discussion



## Oceanic bromine emissions weighted by their ozone depletion potential

S. Tegtmeier et al.

Title Page

Abstract

Introduction

Conclusions

References

Tables

Figures



Back

Close

Full Screen / Esc

Printer-friendly Version

Interactive Discussion



- Dorf, M., Butler, J. H., Butz, A., Camy-Peyret, C., Chipperfield, M. P., Kritten, L., Montzka, S. A., Simmes, B., Weidner, F., and Pfeilsticker, K.: Long-term observations of stratospheric bromine reveal slow down in growth, *Geophys. Res. Lett.*, 33, L24803, doi:10.1029/2006GL027714, 2006.
- 5 Fueglistaler, S., Bonazzola, M., Haynes, P. H., and Peter, T.: Stratospheric water vapor predicted from the Lagrangian temperature history of air entering the stratosphere in the tropics, *J. Geophys. Res.*, 110, D08107, doi:10.1029/2004JD005516, 2005.
- Gettelman, A., Salby, M. L., and Sassi, F., Distribution and influence of convection in the tropical tropopause region, *J. Geophys. Res.*, 107, ACL 6-1–ACL 6-12, doi:10.1029/2001JD001048, 2002.
- 10 Harris, N. R. P. (lead author), Wuebbles, D. J. (lead author), Daniel, J. S., Hu, J., Kujipers, L. J. M., Law, K. S., Prather, M. J., and Schofield, R.: Scenarios and Information for Policymakers, Chapt. 5, in: *Scientific Assessment of Ozone Depletion: 2014, Global Ozone Research and Monitoring Project–Report No. 55*, World Meteorological Organization, Geneva, Switzerland, 2014.
- 15 Hepach, H., Quack, B., Ziska, F., Fuhlbrügge, S., Atlas, E. L., Krüger, K., Peeken, I., and Wallace, D. W. R.: Drivers of diel and regional variations of halocarbon emissions from the tropical North East Atlantic, *Atmos. Chem. Phys.*, 14, 1255–1275, doi:10.5194/acp-14-1255-2014, 2014.
- 20 Hossaini, R., Chipperfield, M. P., Dhomse, S., Ordóñez, C., Saiz-Lopez, A., Abraham, N. L., Archibald, A., Braesicke, P., Telford, P., Warwick, N., Yang, X., and Pyle, J.: Modelling future changes to the stratospheric source gas injection of biogenic bromocarbons, *Geophys. Res. Lett.*, 39, L20813, doi:10.1029/2012GL053401, 2012.
- Hossaini, R., Mantle, H., Chipperfield, M. P., Montzka, S. A., Hamer, P., Ziska, F., Quack, B., Krüger, K., Tegtmeier, S., Atlas, E., Sala, S., Engel, A., Bönisch, H., Keber, T., Oram, D., Mills, G., Ordóñez, C., Saiz-Lopez, A., Warwick, N., Liang, Q., Feng, W., Moore, F., Miller, B. R., Marécal, V., Richards, N. A. D., Dorf, M., and Pfeilsticker, K.: Evaluating global emission inventories of biogenic bromocarbons, *Atmos. Chem. Phys.*, 13, 11819–11838, doi:10.5194/acp-13-11819-2013, 2013.
- 25 30 Kay, J. E., Hillman, B., Klein, S., Zhang, Y., Medeiros, B., Gettelman, G., Pincus, R., Eaton, B., Boyle, J., Marchand, R., and Ackerman, T.: Exposing global cloud biases in the Community Atmosphere Model (CAM) using satellite observations and their corresponding instrument simulators, *J. Climate*, 25, 5190–5207, 2012.

**Oceanic bromine emissions weighted by their ozone depletion potential**

S. Tegtmeier et al.

Title Page

Abstract

Introduction

Conclusions

References

Tables

Figures



Back

Close

Full Screen / Esc

Printer-friendly Version

Interactive Discussion



- Krüger, K., Tegtmeier, S., and Rex, M.: Long-term climatology of air mass transport through the Tropical Tropopause Layer (TTL) during NH winter, *Atmos. Chem. Phys.*, 8, 813–823, doi:10.5194/acp-8-813-2008, 2008.
- Leedham, E. C., Hughes, C., Keng, F. S. L., Phang, S.-M., Malin, G., and Sturges, W. T.: Emission of atmospherically significant halocarbons by naturally occurring and farmed tropical macroalgae, *Biogeosciences*, 10, 3615–3633, doi:10.5194/bg-10-3615-2013, 2013.
- Liang, Q., Stolarski, R. S., Kawa, S. R., Nielsen, J. E., Douglass, A. R., Rodriguez, J. M., Blake, D. R., Atlas, E. L., and Ott, L. E.: Finding the missing stratospheric Br<sub>y</sub>: a global modeling study of CHBr<sub>3</sub> and CH<sub>2</sub>Br<sub>2</sub>, *Atmos. Chem. Phys.*, 10, 2269–2286, doi:10.5194/acp-10-2269-2010, 2010.
- Liang, Q., Atlas, E., Blake, D., Dorf, M., Pfeilsticker, K., and Schauffler, S.: Convective transport of very short lived bromocarbons to the stratosphere, *Atmos. Chem. Phys.*, 14, 5781–5792, doi:10.5194/acp-14-5781-2014, 2014.
- Montzka, S. A., Reimann, S., Engel, A., Krüger, K., O'Doherty, S. J., and Sturges, W. T.: Ozone-depleting substances (ODSs) and related chemicals, in: *Scientific Assessment of Ozone Depletion: 2010*, Rep. 52, chapt. 1, Global Ozone Res., and Monit. Proj., World Meteorol. Organ., Geneva, Switzerland, 1–112, 2011.
- Neale, R. B., Richter, J. H., and Jochum, M.: The impact of convection on ENSO: from a delayed oscillator to a series of events, *J. Climate*, 21, 5904–5924, 2008.
- Neale, R. B., Richter, J. H., Conley, A. J., Park, S., Lauritzen, P. H., Gettelman, A., Williamson, D. L., Rasch, P. J., Vavrus, S. J., Taylor, M. A., Collins, W. D., Zhang, M., and Lin, S.-J.: Description of the NCAR Community Atmosphere Model (CAM5.0), NCAR Tech. Rep. NCAR/TN-486+STR, Natl. Cent. for Atmos. Res., Boulder, Colorado, 268 pp., 2010.
- Nightingale, P. D., Malin, G., Law, C. S., Watson, A. J., Liss, P. S., Liddicoat, M. I., Boutin, J., and Upstill-Goddard, R. C.: In situ evaluation of air–sea gas exchange parameterizations using novel conservative and volatile tracers, *Global Biogeochem. Cy.*, 14, 373–387, doi:10.1029/1999GB900091, 2000.
- Pisso, I., Haynes, P. H., and Law, K. S.: Emission location dependent ozone depletion potentials for very short-lived halogenated species, *Atmos. Chem. Phys.*, 10, 12025–12036, doi:10.5194/acp-10-12025-2010, 2010.
- Pyle, J. A., Warwick, N., Yang, X., Young, P. J., and Zeng, G.: Climate/chemistry feedbacks and biogenic emissions, *Philos. T. R. Soc. A*, 365, 1727–1740, doi:10.1098/rsta.2007.2041, 2007.



**Oceanic bromine emissions weighted by their ozone depletion potential**

S. Tegtmeier et al.

[Title Page](#)[Abstract](#)[Introduction](#)[Conclusions](#)[References](#)[Tables](#)[Figures](#)[Back](#)[Close](#)[Full Screen / Esc](#)[Printer-friendly Version](#)[Interactive Discussion](#)

Quack, B., Atlas, E., Petrick, G., and Wallace, D. W. R.: Bromoform and dibromomethane above the Mauritanian upwelling: atmospheric distributions and oceanic emissions, *J. Geophys. Res.*, 112, D09312, doi:10.1029/2006JD007614, 2007.

Ravishankara, A. R., Daniel, J. S., and Portmann, R. W.: Nitrous oxide (N<sub>2</sub>O): the dominant ozone-depleting substance emitted in the 21st century, *Science*, 326, 123–125, 2009.

Sala, S., Bönisch, H., Keber, T., Oram, D. E., Mills, G., and Engel, A.: Deriving an atmospheric budget of total organic bromine using airborne in situ measurements from the western Pacific area during SHIVA, *Atmos. Chem. Phys.*, 14, 6903–6923, doi:10.5194/acp-14-6903-2014, 2014.

Sinnhuber, B.-M., Sheode, N., Sinnhuber, M., Chipperfield, M. P., and Feng, W.: The contribution of anthropogenic bromine emissions to past stratospheric ozone trends: a modelling study, *Atmos. Chem. Phys.*, 9, 2863–2871, doi:10.5194/acp-9-2863-2009, 2009.

Sioris, C. E., Kovalenko, L. J., McLinden, C. A., Salawitch, R. J., Van Roozendaal, M., Goutail, F., Dorf, M., Pfeilsticker, K., Chance, K., von Savigny, C., Liu, X., Kurosu, T. P., Pomereau, J.-P., Bösch, H., and Frerick, J.: Latitudinal and vertical distribution of bromine monoxide in the lower stratosphere from Scanning Imaging Absorption Spectrometer for Atmospheric Chartography limb scattering measurements, *J. Geophys. Res.*, 111, D14301, doi:10.1029/2005JD006479, 2006.

Solomon, S., Mills, M., Heidt, L. E., Pollock, W. H., and Tuck, A. F.: On the evaluation of ozone depletion potentials, *J. Geophys. Res.*, 97, 825–842, 1992.

Taylor, K. E., Stouffer, R. J., and Meehl, G. A.: The CMIP5 experiment design, *B. Am. Meteorol. Soc.*, 93, 485–498, 2012.

Tegtmeier, S., Krüger, K., Quack, B., Atlas, E. L., Pisso, I., Stohl, A., and Yang, X.: Emission and transport of bromocarbons: from the West Pacific ocean into the stratosphere, *Atmos. Chem. Phys.*, 12, 10633–10648, doi:10.5194/acp-12-10633-2012, 2012.

Velders, G. J. M., Andersen, S. O., Daniel, J. S., Fahey, D. W., and McFarland, M.: The importance of the Montreal Protocol in protecting climate, *P. Natl. Acad. Sci. USA*, 104, 814–819, doi:10.1073/pnas.0610328104, 2007.

Warwick, N. J., Pyle, J. A., Carver, G. D., Yang, X., Savage, N. H., O'Connor, F. M., and Cox, R. A.: Global modeling of biogenic bromocarbons, *J. Geophys. Res.*, 111, D24305, doi:10.1029/2006JD007264, 2006.

Wuebbles, D. J.: Chlorocarbon emission scenarios: potential impact on stratospheric ozone, *J. Geophys. Res.*, 88, 1433–1443, 1983.

Wuebbles, D. J., Patten, K., Johnson, M., and Kotamarthi, R.: New methodology for ozone depletion potentials of short-lived compounds: n-propyl bromide as an example, *J. Geophys. Res.*, 106, 14551–14571, 2001.

5 Yang, X., Abraham, N. L., Archibald, A. T., Braesicke, P., Keeble, J., Telford, P. J., Warwick, N. J., and Pyle, J. A.: How sensitive is the recovery of stratospheric ozone to changes in concentrations of very short-lived bromocarbons?, *Atmos. Chem. Phys.*, 14, 10431–10438, doi:10.5194/acp-14-10431-2014, 2014.

10 Ziska, F., Quack, B., Abrahamsson, K., Archer, S. D., Atlas, E., Bell, T., Butler, J. H., Carpenter, L. J., Jones, C. E., Harris, N. R. P., Hepach, H., Heumann, K. G., Hughes, C., Kuss, J., Krüger, K., Liss, P., Moore, R. M., Orlikowska, A., Raimund, S., Reeves, C. E., Reifenhäuser, W., Robinson, A. D., Schall, C., Tanhua, T., Tegtmeier, S., Turner, S., Wang, L., Wallace, D., Williams, J., Yamamoto, H., Yvon-Lewis, S., and Yokouchi, Y.: Global sea-to-air flux climatology for bromoform, dibromomethane and methyl iodide, *Atmos. Chem. Phys.*, 13, 8915–8934, doi:10.5194/acp-13-8915-2013, 2013.

**Oceanic bromine emissions weighted by their ozone depletion potential**

S. Tegtmeier et al.

Title Page

Abstract

Introduction

Conclusions

References

Tables

Figures



Back

Close

Full Screen / Esc

Printer-friendly Version

Interactive Discussion





**Oceanic bromine emissions weighted by their ozone depletion potential**

S. Tegtmeier et al.

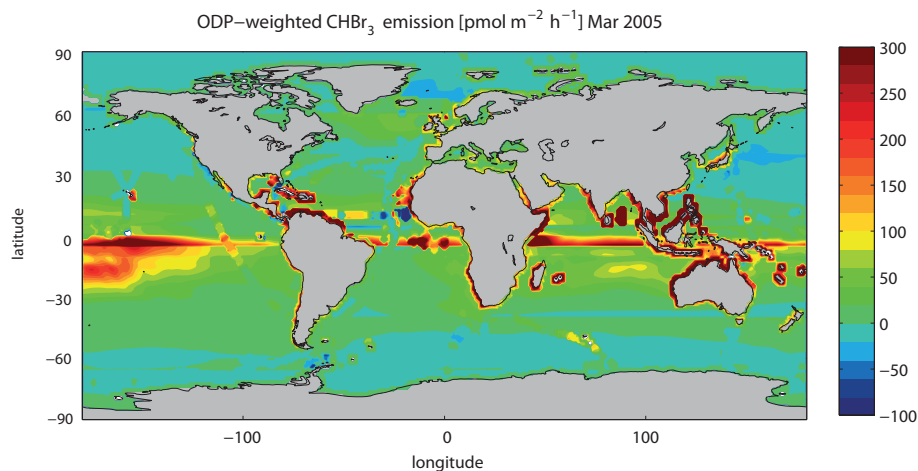


**Figure 2.** Global ODP-weighted  $\text{CHBr}_3$  emissions are given for March 2005. The ODP-weighted emissions have been calculated by multiplying the  $\text{CHBr}_3$  emissions with the ODP at each grid point.

[Title Page](#)[Abstract](#)[Introduction](#)[Conclusions](#)[References](#)[Tables](#)[Figures](#)[Back](#)[Close](#)[Full Screen / Esc](#)[Printer-friendly Version](#)[Interactive Discussion](#)



**Oceanic bromine emissions weighted by their ozone depletion potential**

S. Tegtmeier et al.

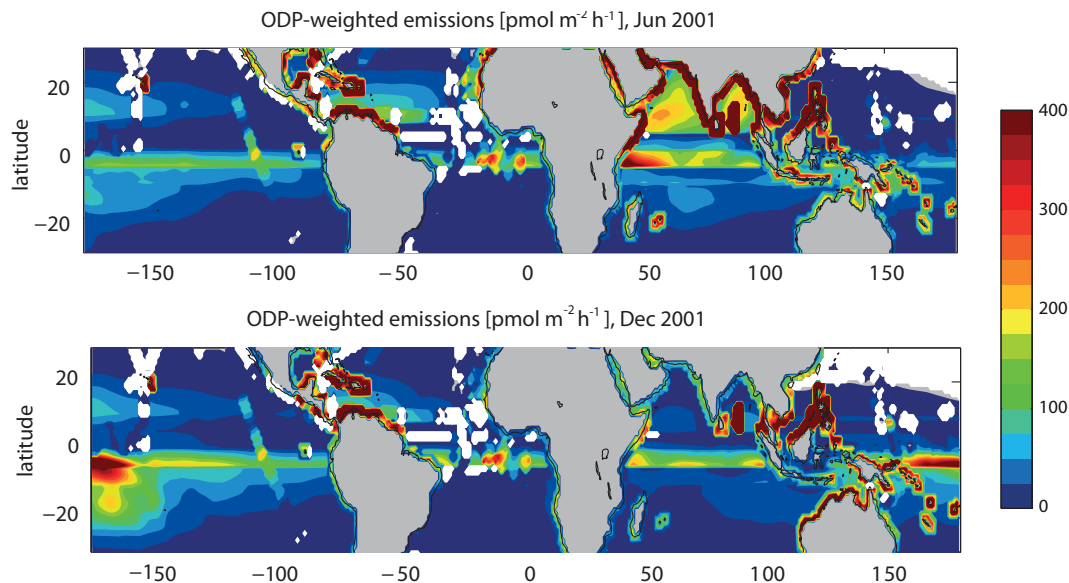


**Figure 4.** ODP-weighted emissions calculated as the product of the emissions maps (not show here) and the trajectory-based ODP fields (Fig. 5a) are displayed for June and December 2001.

[Title Page](#)[Abstract](#)[Introduction](#)[Conclusions](#)[References](#)[Tables](#)[Figures](#)[◀](#)[▶](#)[◀](#)[▶](#)[Back](#)[Close](#)[Full Screen / Esc](#)[Printer-friendly Version](#)[Interactive Discussion](#)

## Oceanic bromine emissions weighted by their ozone depletion potential

S. Tegtmeier et al.

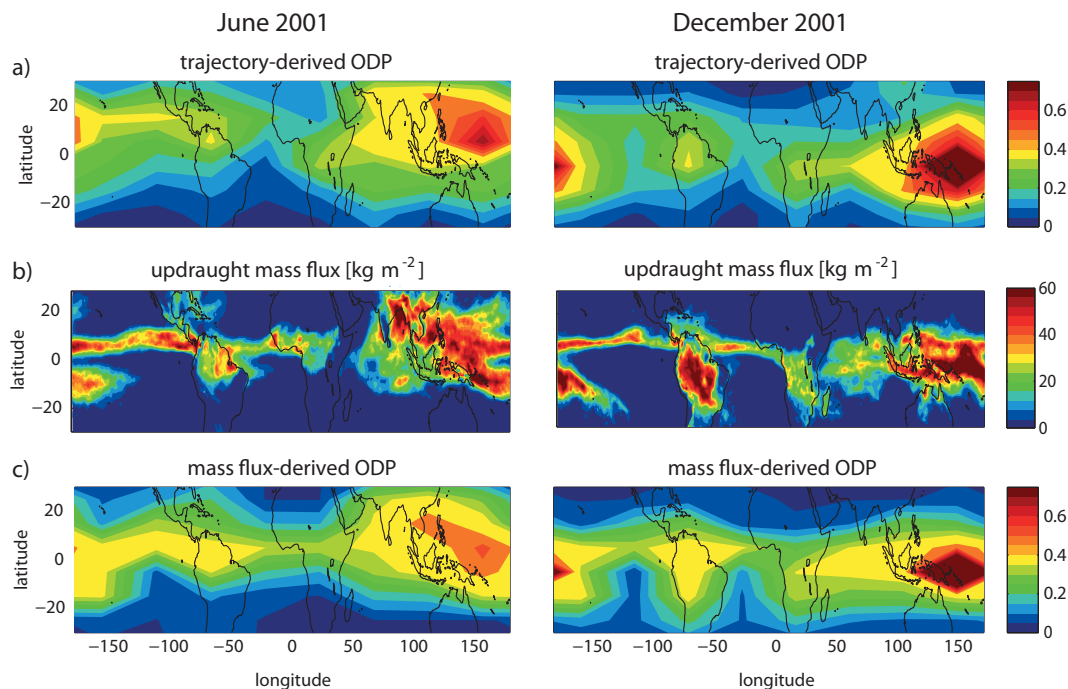


**Figure 5.** Trajectory-based ODP fields **(a)**, monthly mean ERA-Interim updraught mass flux between 250 and 80 hPa **(b)**, and the mass flux-derived ODP **(c)** are displayed for June and December 2001.

[Title Page](#)[Abstract](#)[Introduction](#)[Conclusions](#)[References](#)[Tables](#)[Figures](#)[◀](#)[▶](#)[◀](#)[▶](#)[Back](#)[Close](#)[Full Screen / Esc](#)[Printer-friendly Version](#)[Interactive Discussion](#)



**Oceanic bromine emissions weighted by their ozone depletion potential**

S. Tegtmeier et al.

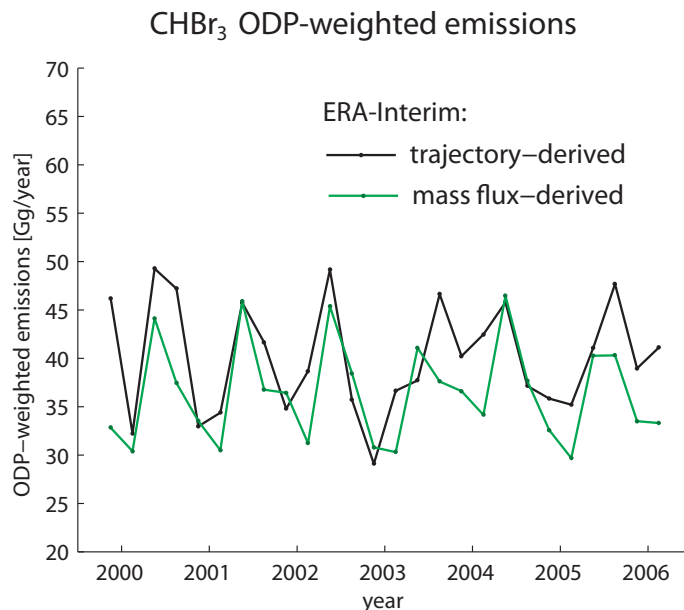


**Figure 6.** Time series of ODP-weighted CHBr<sub>3</sub> emissions based on ERA-Interim trajectory-derived ODP (black line) and mass flux-derived ODP (green line) for March, June, September and December 1999 to 2006.

[Title Page](#)[Abstract](#)[Introduction](#)[Conclusions](#)[References](#)[Tables](#)[Figures](#)[◀](#)[▶](#)[◀](#)[▶](#)[Back](#)[Close](#)[Full Screen / Esc](#)[Printer-friendly Version](#)[Interactive Discussion](#)

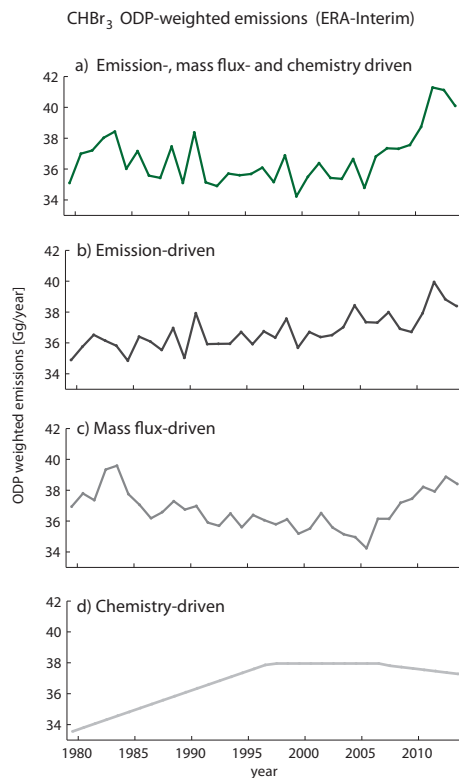


**Figure 7.** Time series of ODP-weighted CHBr<sub>3</sub> emissions for 1979–2013 based on ERA-Interim mass flux-derived ODP is shown **(a)**. Additionally, sensitivity studies are displayed where two factors are kept constant at their respective 1979–013 mean values, while the other factor varies with time. The sensitivity studies include ODP-weighted CHBr<sub>3</sub> emissions driven by time-varying emissions **(b)**, time-varying mass flux-derived ODP **(c)**, and time-varying stratospheric chemistry **(d)**.

**Oceanic bromine emissions weighted by their ozone depletion potential**

S. Tegtmeier et al.

Title Page	
Abstract	Introduction
Conclusions	References
Tables	Figures
◀	▶
◀	▶
Back	Close
Full Screen / Esc	
Printer-friendly Version	
Interactive Discussion	



## Oceanic bromine emissions weighted by their ozone depletion potential

S. Tegtmeier et al.

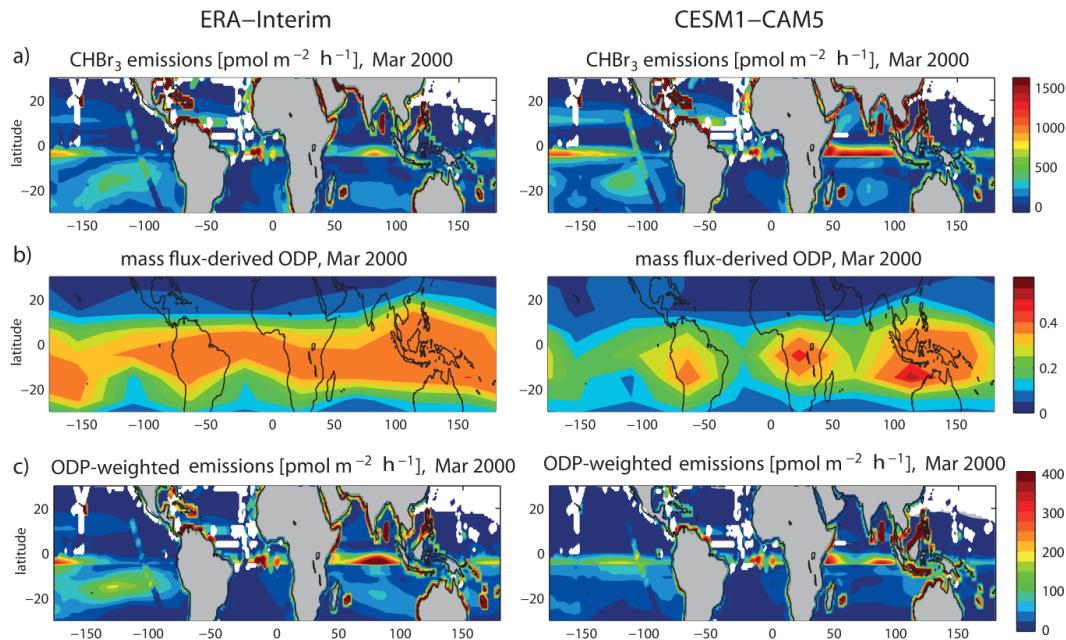


**Figure 8.** CHBr<sub>3</sub> emissions (a), mass flux-derived ODP (b) and ODP-weighted CHBr<sub>3</sub> emissions (c) are shown for ERA-Interim and for CESM1-CAM5 for March 2000.

[Title Page](#)
[Abstract](#)
[Introduction](#)
[Conclusions](#)
[References](#)
[Tables](#)
[Figures](#)
[Back](#)
[Close](#)
[Full Screen / Esc](#)
[Printer-friendly Version](#)
[Interactive Discussion](#)

**Oceanic bromine emissions weighted by their ozone depletion potential**

S. Tegtmeier et al.

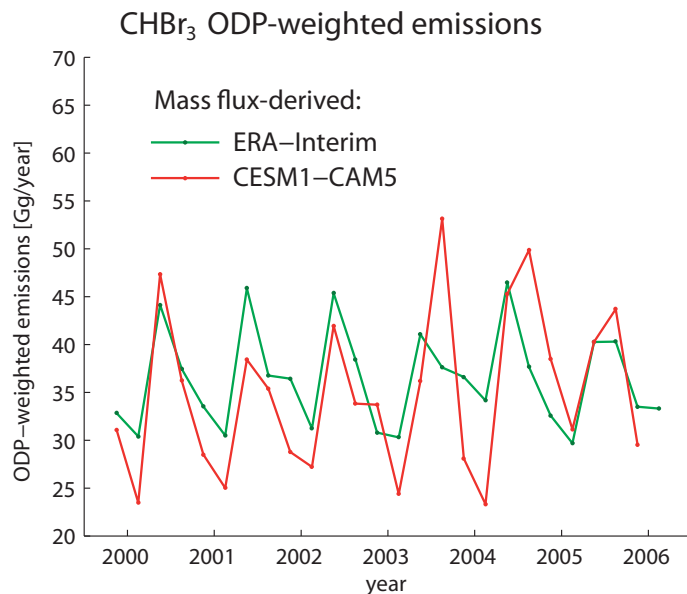


**Figure 9.** Time series of ODP-weighted CHBr<sub>3</sub> emissions based on ERA-Interim (green line) and on historical CESM1-CAM5 runs (red line) are shown. The ODP is calculated from the updraught mass flux fields.

[Title Page](#)[Abstract](#)[Introduction](#)[Conclusions](#)[References](#)[Tables](#)[Figures](#)[◀](#)[▶](#)[◀](#)[▶](#)[Back](#)[Close](#)[Full Screen / Esc](#)[Printer-friendly Version](#)[Interactive Discussion](#)

## Oceanic bromine emissions weighted by their ozone depletion potential

S. Tegtmeier et al.

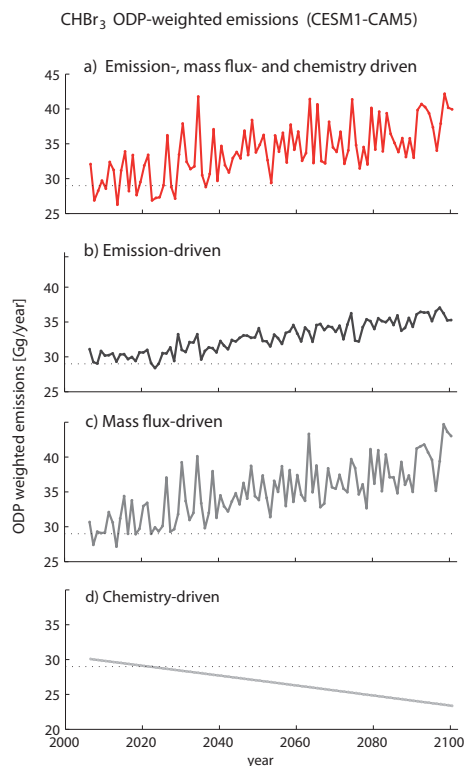


**Figure 10.** Time series of ODP-weighted CHBr<sub>3</sub> emissions for 2006–2100 based on future (RCP8.5 scenario) CESM1-CAM5 runs are shown **(a)**. Additionally, sensitivity studies are displayed where two factors are kept constant at their respective 2006–2015 mean values, while the other factor varies with time. The sensitivity studies include ODP-weighted CHBr<sub>3</sub> emissions driven by time-varying emissions **(b)**, time-varying mass flux-derived ODP **(c)**, and time-varying stratospheric chemistry **(d)**.

## Oceanic bromine emissions weighted by their ozone depletion potential

S. Tegtmeier et al.

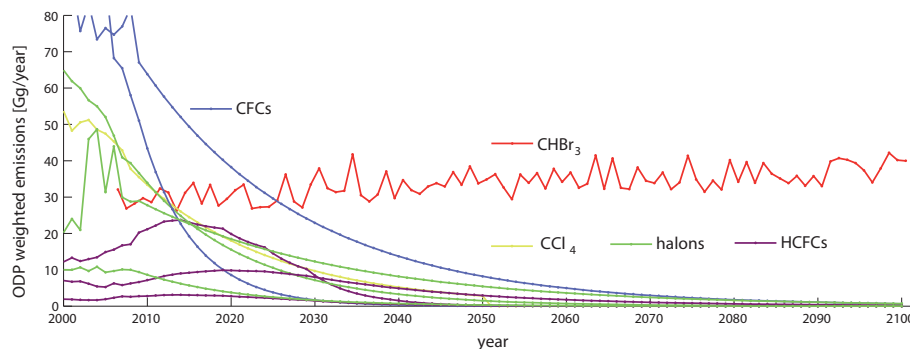


**Figure 11.** Future projections of ODP-weighted emissions of  $\text{CHBr}_3$  and other long-lived halocarbons are shown for 2000–2100. Future ODP-weighted emission estimates for long-lived halocarbons (halons: halon 1211, 1301, 2402; HCFCs: HCFC-22, -141, -142) are shown.

[Title Page](#)[Abstract](#)[Introduction](#)[Conclusions](#)[References](#)[Tables](#)[Figures](#)[◀](#)[▶](#)[◀](#)[▶](#)[Back](#)[Close](#)[Full Screen / Esc](#)[Printer-friendly Version](#)[Interactive Discussion](#)